ACS Biomaterials SCIENCE & ENGINEERING

Article

pubs.acs.org/journal/abseba

Nanogel-Mediated RNAi Against Runx2 and Osx Inhibits Osteogenic Differentiation in Constitutively Active BMPR1A Osteoblasts

Arun R. Shrivats,[†,‡] Michael C. McDermott,[†] Molly Klimak,[†] Saadyah E. Averick,[§,#] Haichun Pan,[⊥] Krzysztof Matyjaszewski,[§] Yuji Mishina,[⊥] and Jeffrey O. Hollinger*[,†]

[†]Department of Biomedical Engineering, Carnegie Mellon University, 700 Technology Drive, Pittsburgh, Pennsylvania 15219, United States

[§]Department of Chemistry, Carnegie Mellon University, 4400 Fifth Avenue, Pittsburgh, Pennsylvania 15213, United States

[⊥]School of Dentistry, University of Michigan, 1011 North University Avenue, Ann Arbor, Michigan 48109, United States

Supporting Information

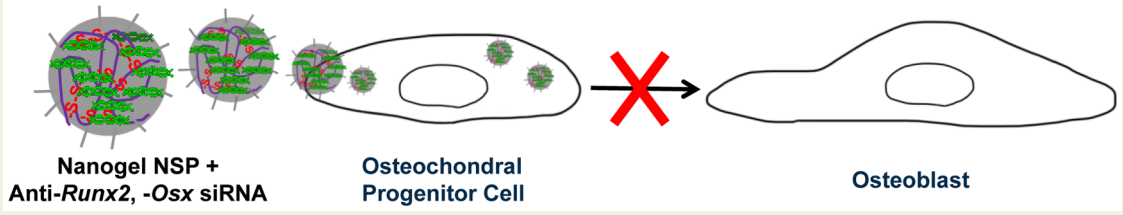

ABSTRACT: Trauma-induced heterotopic ossification (HO) and fibrodysplasia ossificans progressiva (FOP) are acquired and genetic variants of pathological bone formation occurring in soft tissues. Conventional treatment modalities target the inflammatory processes preceding bone formation. We investigated the development of a prophylaxis for heterotopic bone formation by addressing the biological basis for HO − dysregulation in the bone morphogenetic protein (BMP) signaling pathway. We previously reported the synthesis of cationic nanogel nanostructured polymers (NSPs) for efficient delivery of short interfering ribonucleic acids (siRNAs) and targeted gene silencing. Results suggested that nanogel:siRNA weight ratios of 1:1 and 5:1 silenced *Runx2* and *Osx* gene expression in primary mouse osteoblasts with a constitutively active (ca) BMP Receptor 1A (BMPR1A) by the Q233D mutation. Repeated RNAi treatments over 14 days significantly inhibited alkaline phosphatase activity in caBMPR1A osteoblasts. Hydroxyapatite (HA) deposition was diminished over 28 days in culture, though complete suppression of HA deposition was not achieved. Outcome data suggested minimal cytotoxicity of nanogel-based RNAi therapeutics, and the multistage disruption of BMP-induced bone formation processes. This RNAi based approach to impeding osteoblastic differentiation and subsequent bone formation may form the basis of a clinical therapy for heterotopic bone formation.

KEYWORDS: *atom transfer radical polymerization, gene delivery, siRNA, bone morphogenetic protein, heterotopic ossification, fibrodysplasia ossificans progressiva*

INTRODUCTION

Heterotopic ossification (HO) is defined as the formation of lamellar bone in soft tissue, typically as a sequela to polytrauma, and is a compelling clinical concern in both military and civilian medicine.[1−4] Fibrodysplasia ossificans progressiva (FOP) is a rare disease characterized by the progressive bone formation in soft tissues over the patient's lifetime, resulting in restricted mobility and early mortality.[5,6] Both traumatic and congenital cases of heterotopic bone formation may be attributed to dysregulation in bone morphogenetic protein (BMPs) signaling. BMPs are a potent group of morphogens responsible for bone formation, maintenance, and repair.[7] In trauma-induced HO patients, the putative mechanism for bone formation is by increased expression of BMPs.[8] In FOP patients, an autosomal dominant mutation, typically R206H, induces hyperactivity of ACVR1 (a type I BMP receptor) causing dysregulated BMP signals at a cellular level.[9] Increased BMP-2 and BMP-4 levels have been found in fibromatous lesions of FOP patients.[10] These facts underscore a critical contribution of BMP signaling during pathogenesis in trauma-induced HO and FOP patients.

There are limited treatment options for HO; contemporary treatments include administration of nonsteroidal anti-inflammatory drugs (NSAIDs) or corticosteroids, and radiotherapy, though there are adverse effects associated with each of these treatment courses.[11−13] In HO patients, surgical excision of heterotopic bone runs the risk of HO recurrence at the surgical site, whereas in FOP patients, surgery-induced trauma induces explosive bone regrowth.[14] There is a compelling clinical need for therapeutics that may prevent heterotopic bone formation.

Received: July 11, 2015
Accepted: September 25, 2015

DOI: 10.1021/acsbiomaterials.5b00294
ACS Biomater. Sci. Eng. XXXX, XXX, XXX−XXX

Harnessing RNA interference machinery, the delivery of short interfering RNAs (siRNA) against the osteogenic cascade may produce a prophylaxis for heterotopic bone formation. This strategy may avoid many of the adverse side effects associated with contemporary HO therapeutic interventions. There are several key challenges in the therapeutic delivery of siRNA that must be overcome, including nuclease degradation of siRNA, electrostatic repulsion of siRNA by cell membranes, and toxicity of siRNA delivery systems.[15] The advent of modern polymerization techniques has enabled the production of polymers with a wide range of monomers, architectures, and stimuli-responsive behavior.[16−18] We have produced cationic nanogel nanostructured polymers (nanogel NSPs) by atom transfer radical polymerization (ATRP) to produce a bioresponsive, interconnected polymeric network for siRNA delivery.[19] This effort integrates several strategies for efficient siRNA delivery, including PEGylation, steric shielding of siRNAs, built-in features for endosomal escape, and stimuli-specific degradation mechanisms. We previously reported that nanogel NSPs demonstrate minimal dose-dependent cytotoxicity, efficient siRNA binding and release, and internalization into mammalian cells.[20,21] Endosomal escape features were not directly evaluated, though they are inferred as a plausible mechanism behind successful nanogel-mediated gene delivery based on the DMAEMA core.[22] Targeted gene knockdown capabilities were confirmed in both insect and mammalian cell lines.[20,21] We also recently demonstrated successful nanogel-mediated gene silencing in vivo, against *Gfp* expression in a mouse model.[23] In doing so, the nanogel NSP delivery platform has overcome several traditional limitations to polymeric siRNA delivery, including cytotoxicity and efficient siRNA delivery in the presence of serum.

In designing a prophylaxis for prevention of heterotopic bone formation, we target the biological basis for HO—dysregulation in BMP signaling. The BMP signaling pathway contains several molecular agents that are viable targets for interference; of particular note are the transcription factors Runt related transcription factor 2 (RUNX2) and Osterix (OSX), which are expressed within 48 h of BMP-induced differentiation in culture.[24,25] Both transcription factors are master regulators of bone formation and mark the point of convergence of multiple bone-forming pathways.[25−29] Furthermore, genetic disruption of either *Runx2* or *Osx* has led to the complete absence of bone formation.[28,29] This approach, targeted against *Runx2* and *Osx*, may reduce gene expression and impede osteogenic differentiation. Recent efforts to prevent HO have underscored the importance of *Runx2* and *Osx* gene expression in bone formation pathways, and provide a benchmark for the evaluation of nanogel NSP-mediated siRNA delivery. Adenoviral delivery of *Runx2* siRNA has mitigated indications of HO in both in vitro and in vivo models.[30] Liposomal carriers have also been employed to silence *Runx2*, with success in preventing downstream osteogenic marker expression in the presence of BMP-2 in myoblast cell lines.[31] The development of appropriate treatment conditions may enable nanogel NSP-mediated knockdown of *Runx2* and *Osx*. We hypothesize this may inhibit the osteogenic signaling cascade, ultimately attenuating hydroxyapatite deposition in vitro.

To evaluate the potential for nanogel-mediated RNAi treatments against HO and FOP, we must employ appropriate testing environments. A proper in vitro evaluation of RNAi therapeutics against rogue ossification should be conducted in cell culture models with fidelity to the HO pathology. In this study, we evaluated RNAi therapeutics in primary osteoblasts harvested from a transgenic mouse line with an inducible constitutively active (ca) BMP Receptor, Type 1A (BMPR1A) via the Q233D mutation (caBMPR1A^{Q233D} osteoblasts).[32,33] BMPR1A plays a key role in regulation of signals for osteogenic differentiation and is the preferred receptor for BMP-2/4 ligands.[34] Due to the mutation of Q233D, the receptor transduces robust levels of BMP signaling without ligands and caBMPR1A^{Q233D} osteoblasts treated with BMP-2 demonstrate a further increased levels of BMP signaling leading to higher expression of osteoblastic markers than BMP-2 treated control osteoblasts.[33] As such, they provide a representative in vitro arena for the testing of RNAi therapeutics for pathologies characterized by rogue bone formation.

Here, we report a framework for the optimization of a promising polymeric approach for siRNA delivery, using trauma-induced HO and FOP as a testing environment. Key delivery parameters included NSP:siRNA ratios, siRNA doses, as well as timing considerations against transcriptional targets *Runx2* and *Osx*. After optimization, RNAi treatments induced targeted gene silencing of *Runx2* and *Osx* in caBMPR1A^{Q233D} osteoblasts during rhBMP-2-induced differentiation. Temporal and dosing parameters for siRNA delivery were determined to achieve peak silencing of target genes during differentiation. As expected, *Runx2* and *Osx* knockdown propagated to alkaline phosphatase mRNA (*Alp*) and protein (ALP) expression—a strong indicator of the efficient nature of nanogel-mediated siRNA delivery and subsequent gene silencing. Over 28 days, RNAi treatments against *Runx2* and *Osx* inhibited hydroxyapatite deposition characteristic of late-stage osteoblastic differentiation. Together with the very low cytotoxicity of nanogel-based RNAi treatments, the in vitro success demonstrated here to attenuate expression of early-, mid-, and late-stage osteoblast differentiation markers should provide insight into develop a nonviral RNAi therapeutic for HO in the clinic using nanogel NSPs for siRNA delivery.

MATERIALS & METHODS

Cell Culture. Generation of inducible caBmpr1a mice was reported previously.[32,33] *caBmpr1a* mice were bred with P0-Cre[35] to activate *caBmpr1a* gene expression in a neural crest-specific manner and primary osteoblasts (both caBMPR1A^{Q233D} and wild-type) were harvested from frontal bones of newborn mouse calvaria.[33] Osteoblasts were cultured in alpha-minimum essential medium (αMEM) supplemented with 10% fetal bovine serum (ATCC, Manassas, VA, 30−2020) and 1% penicillin/streptomycin (ATCC, 30−2300). When required, cells were passaged with 0.25% trypsin EDTA (Life Technologies, Carlsbad, CA, 25200−056). All cells used for experiments were at passage 4 or lower. To evaluate levels of BMP-Smad signaling, isolated osteoblasts were cultured with or without rhBMP2 at 100 ng/mL for 30 min. Levels of phospho-Smad1/5/8 were measured by Western blot using a rabbit antiphospho-SMAD1/5/8 (pSMAD1/5/8) (1:1000, 9511, Cell Signaling) (Figure S1).

Nanogel NSP Synthesis. Cationic nanogels were prepared by activators generated by electron transfer atom transfer radical polymerization (AGET ATRP) in inverse miniemulsion by copolymerizing quaternized dimethyl aminoethyl methacrylate (qDMAEMA), oligo(ethylene oxide) methacrylate (OEOMA, M_n = 300), and a water-soluble disulfide methacrylate cross-linker with a poly(ethylene glycol 2−bromoisobutyrate) initiator and a copper bromide tris(2-(dimethylamino)ethyl)amine catalyst system dissolved in water (Figure S2). The inverse miniemulsion was prepared by ultrasonication of the aqueous phase in a cyclohexane Span80 solution. After the reaction mixture was degassed an ascorbic acid solution was injected to generate the active catalyst. The cationic nanogels were

DOI: 10.1021/acsbiomaterials.5b00294
ACS Biomater. Sci. Eng. XXXX, XXX, XXX−XXX

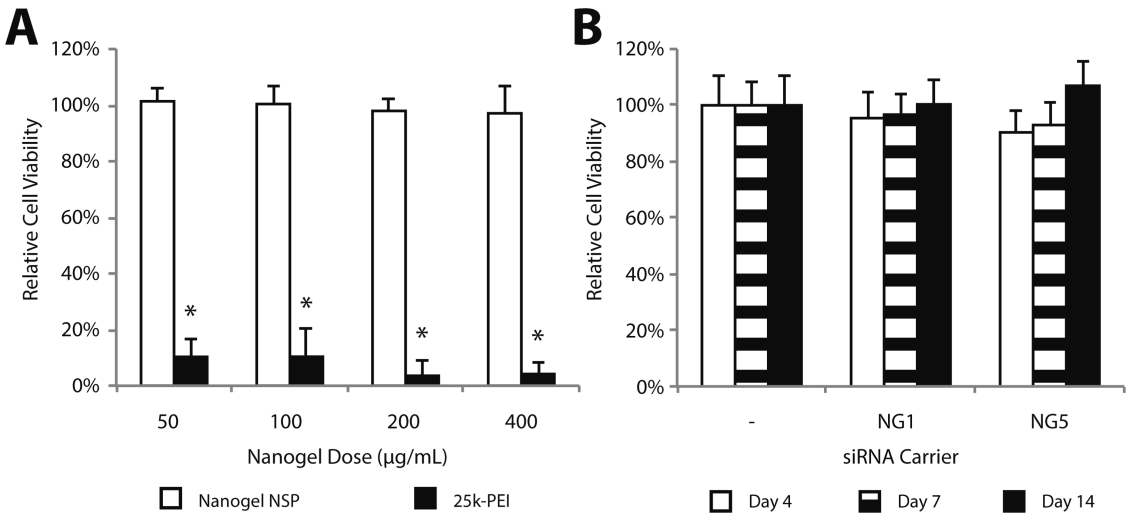

Figure 1. Cytotoxicity of nanogel NSPs and RNAi treatment doses. (A) MTS-based NSP toxicity assessment in primary mouse WT osteoblasts indicated that nanogel doses up to 400 μg/mL (per 50 000 cells) did not significantly alter cell viability over 24 h. As expected, the delivery of 25k-polyethylenimine (PEI) produced significant reductions in cell viability at all concentrations above 50 μg/mL. (B) Analysis of osteoblast proliferation after 4, 7, and 14 days of receiving nanogel RNAi treatments (refreshed every 48 h) via the Picogreen assay revealed no significant differences in DNA content after delivery of siRNAs at 1:1 (NG1) and 5:1 (NG5) ratios at 30 nM concentrations. Data reported as means ((A) $n = 4$; (B) $n = 8$) + standard deviations; statistical significance indicated where $p < 0.05$.

purified using dialysis and were characterized using dynamic light scattering and zeta potential analysis. Further details on nanogel NSP synthesis and characterization can be found in the following reference.[19]

NSP Toxicity. The CellTiter 96 Aqueous One Solution Cell Proliferation MTS Assay (Promega, Madison, WA, G5421) was employed to quantify mitochondrial enzyme activity after 2 days in primary mouse osteoblasts. Cells were seeded at 25 000 cells/mL in 96-well plates (0.2 mL/well) and cultured overnight prior to polymer delivery. Polymer solutions were prepared at 25 μg/μL and delivered to wells at the reported concentrations. The MTS assay was executed 48 h after treatments, as per the manufacturer's directions. Briefly, existing culture medium was aspirated and replaced with 100 mL fresh complete medium. Twenty μL MTS reagent was added to each well and incubated at 37 °C and 5% CO_2 for 1 h. Sample absorbance was measured at 492 nm using a Tecan SpectraFluor (Tecan, F129003). Absorbance values from media-alone groups were subtracted from all other groups; cohorts receiving polymer doses were normalized to untreated cell cohorts to calculate percent cell viability.

Four-, seven-, and fourteen-day viability studies were conducted using Quant-iT PicoGreen dsDNA Assay (Life Technologies, P7589). Cells were seeded at 15,000 cells/mL in 24-well plates (1 mL/well). Polymer treatments were delivered every 48 h along with fresh culture medium. At experimental end points (days 4, 7, and 14), cells were lysed using Cell Signaling Lysis Buffer (Cell Signaling Technology #9803). PicoGreen-based DNA content was evaluated after combination of 100 μL lysates with 100 μL PicoGreen dye (1:200 dilution in TE buffer) for 3 min in 96-well assay plates. Sample fluorescence was analyzed using a Tecan Spectrafluor (Tecan, F129003) at 492 nm (excitation) and 520 nm (emission) filters.

RNAi Treatment Preparation. Nanogel NSPs, initially prepared as a powder, were dissolved in nuclease-free water (Life Technologies, AM9930) at concentrations ranging from 10 to 50 μg/μL. SiRNA were thawed at room temperature from −20 °C and NSP-siRNA treatments were prepared by mixing nanogel NSPs and siRNAs in weight:weight ratios ranging from 1:1 to 10:1 in volumes up to 25 μL. RNAi formulations were prepared in bulk but stored as individual treatments at −20 °C until their use, when they were thawed and delivered to cell cultures.

Gene Expression. CellsDirectTM One-Step qRT-PCR Kit with ROX (Life Technologies, Carlsbad, CA) and an ABI Prism 7000 Sequence Detection System (Applied Biosystems, Foster City, CA) were used for the analysis of *Runx2* and *Osx* mRNA expression. Cell lysis, RNA extraction, and cDNA preparation were carried out according to the CellsDirectTM One-Step qRT-PCR (Applied Biosystems, Foster City, CA) Kit protocol. Each reaction contained SuperScript III RT/Platinum *Taq* Mix, 2X Reaction Mix with ROX, and Taqman Gene Expression Assay containing predesigned primers, and 4 μL of processed cell lysates. Expression of *Runx2*, *Osx*, and *Alp* were normalized to *Actb* expression using the comparative Ct method. Fold change data was represented as a percent (normalized to rhBMP-2-treated groups), and reported as mean + standard deviation with $n = 8$.

Alkaline Phosphatase Activity. Cells were seeded at 15,000 cells/mL in 24-well plates (1 mL/well). RNAi treatments against *Runx2* were delivered 24 h prior to treatments against *Osx*. Cell culture media was refreshed in conjunction with *Osx* treatments and rhBMP-2 delivery (where applicable). This 48 h cycle was repeated for the duration of the study. At experimental end points (days 4, 7 and 14), cells were lysed using cell signaling lysis buffer (Cell Signaling Technology, Danvers, MA, #9803). ALP activity was measured as previously described.[36]

von Kossa Staining. Cells were seeded at 15 000 cells/mL in 24-well plates (1 mL/well). RNAi treatments against *Runx2* were delivered 24 h prior to treatments against *Osx*. Cell culture media was refreshed in conjunction with *Osx* treatments and rhBMP-2 delivery (where applicable). This 48-h cycle was repeated for the duration of the study. After 28 days in culture (14 RNAi treatment cycles), cells were fixed in 70% ethanol for 15 min at room temperature. 1% silver nitrate was added and samples were exposed to bright white light for 60 min. After rinsing with DI water, samples were treated with 5% sodium thiosulfate for 2 min to minimize nonspecific staining. Samples were imaged using a Zeiss SteREO scope at 48x.

Alizarin Red S Staining. Cell cultures were seeded at 15 000 cells/mL in 24-well plates (1 mL/well) and cultured for 28 days. As previously reported,[36] cells were fixed in ice-cold 70% ethanol for 1 h and rinsed three times with DI water. 40 mM Alizarin Red S stain was added (pH adjusted to 4.2) for 10 min under rotation. After five additional washes with DI water, cells were imaged using a Zeiss SteREO scope at 20×.

OsteoImage Mineralization. An assessment of hydroxyapatite formation in cell cultures was conducted by the OsteoImage Bone Mineralization Assay (Lonza, Walkersville, MD, PA-1503). Cells were seeded at 15,000 cells/mL in 96-well plates (0.2 mL/well). After 7, 14, 21, and 28 days in culture, cells were rinsed with 1× PBS and fixed with 70% ethanol for 20 min. The OsteoImage assay was executed as

DOI: 10.1021/acsbiomaterials.5b00294
ACS Biomater. Sci. Eng. XXXX, XXX, XXX−XXX

per the manufacturer's protocol. Briefly, cells were rinsed twice using the OsteoImage Wash Buffer, stained with the hydroxyapatite dye provided (prepared by 1:100 dilution in the wash buffer) and incubated for 30 min. Following incubation, cells were rinsed three more times with wash buffer and analyzed using a Tecan Spectrafluor (Tecan F129003) at 492 nm (excitation) and 535 nm (emission) filters.

Statistical Analyses. All data are expressed as means ± standard deviations. Sample quantities varied based on experimental setup, and thus, are indicated where appropriate. Statistical differences among experimental cohorts were determined by ANOVA with posthoc Tukey-Kramer analysis for multiple comparisons using Minitab 16 Statistical Software. Statistically significant differences were established at $p < 0.05$.

RESULTS

The successful design of an NSP-RNAi therapeutic to prevent osteogenic differentiation requires evaluation against several key performance criteria. For this platform, key properties determined were the cytotoxicity of RNAi treatments, expression of target genes *Runx2* and *Osx*, as well as expression of downstream osteoblast differentiation markers.

Dose-dependent cytotoxic effects of nanogel NSPs were determined in primary osteoblast cultures over a 14-day temporal period. Initial 48-h testing was conducted using the MTS assay to quantify mitochondrial enzyme activity. Results determined that after 48 h of NSP treatment, nanogel-treated cultures were at 100.6 ± 3.8%, 99.7 ± 5.4%, 97.2 ± 4.1%, and 96.4 ± 9.3% cell viability at NSP doses of 50, 100, 200, and 400 μg/mL, respectively (Figure 1A). Percent viability was determined by normalization to untreated cell cultures. As a comparison, branched polyethylenimine$_{25k}$ (PEI)—a cationic polymer widely used for siRNA delivery—demonstrated cell viability ranging from 9.9% ± 6.0% at 50 μg/mL to 4.1% ± 4.1% at 400 μg/mL. This is an indicator of cytotoxicity, for which PEI is well-known.[37]

Cytotoxicity analyses were extended over a 14-day period by PicoGreen-based DNA quantitation. Here, the dose-dependent impact of nanogel NSPs on cellular proliferation and viability was studied in the context of siRNA delivery. Thirty pmol doses of siRNA (at 30 nM) were delivered by nanogel NSPs at 1:1 and 5:1 ratios. The rationale for selection of these ratios for NSP was based on prior results demonstrating successful gene silencing at these ratios.[20] Results suggested that cells treated with 1:1 NSP:siRNA ratios were approximately 100% viable over a 14-day time course. Cells treated with 5:1 NSP:siRNA ratios demonstrated reduced viability of 90.4 ± 7.4% and 93.0 ± 8.4% at days 4 and 7, respectively. Viability after 14 days in culture was measured at 106.9 ± 8.9%, indicating no significant differences from untreated cell cultures. Nanogel 1:1 treatments demonstrated 4-, 7- and 14-day viability measurements of 95.5 ± 9.2%, 96.7 ± 7.3%, and 100.3 ± 9.1%, respectively. No significant differences were determined in cellular proliferation among untreated cells and those treated with 1:1 and 5:1 RNAi treatments.

caBMPR1A^{Q233D} osteoblasts isolated from newborn calvaria showed robust levels of BMP signaling measured by phospho-SMAD1/5/8 with BMP-2 (Figure S1). The efficacy of nanogel-mediated RNAi attack on *Runx2* expression in caBMPR1A^{Q233D} osteoblasts was determined by quantitative real-time polymerase chain reaction (qRT-PCR) 48 h following the delivery of recombinant human BMP-2 (rhBMP-2); RNAi treatments against *Runx2* were delivered 24 h prior to BMP delivery. Results indicated that nanogel:siRNA weight ratios spanning 1:1 (NG1) to 100:1 (NG100) elicited significant reductions in *Runx2* gene expression (Figure 2A). Peak knockdown was achieved by NG1, NG5 and NG10 treatments, which elicited reductions in *Runx2* expression of 70.3 ± 12.0%, 77.3 ± 7.1, and 62.3 ± 10.7%, respectively ($p < 0.001$). Despite this efficacy, *Runx2* mRNA levels were not knocked down to levels consistent with untreated cells ($p < 0.05$). RNAi treatments

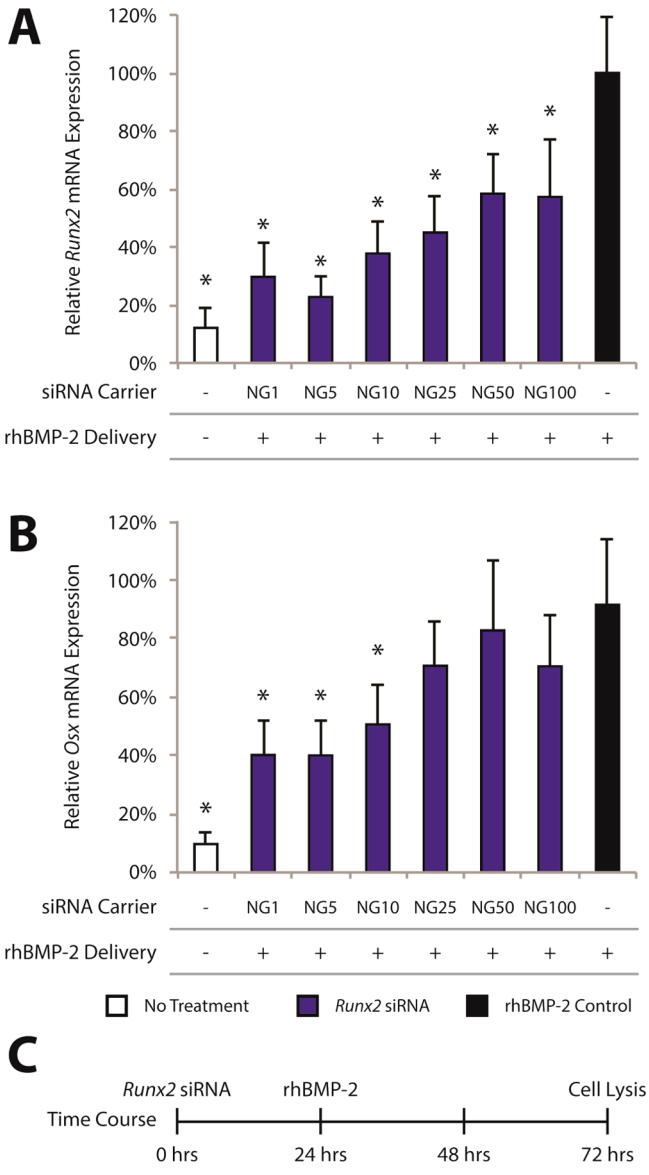

Figure 2. Nanogel ratiometric knockdown of *Runx2* in caBMPR1A osteoblasts with the Q233D mutation (caBMPR1A^{Q233D}) by delivery of *Runx2* siRNAs at 30 nM doses. (A) Nanogel:siRNA ratios ranging from 1:1 (NG1) to 100:1 (NG100) produced significant reductions in *Runx2* gene expression ($p < 0.05$). Delivery of siRNAs between NG1 and NG10 ratios resulted in peak *Runx2* mRNA. Data reported as means ($n = 6$) + standard deviations. (B) Knockdown of *Osx* gene expression as a consequence of RNAi targeting of *Runx2*. Results indicated that targeting *Runx2* by NSP:siRNA ratios from NG1 to NG10 produces a significant reduction in expression of the downstream *Osx* gene. Data reported as means ($n = 6$) + standard deviations. (C) Schematic of experimental time course. siRNA delivery against *Runx2* preceded rhBMP-2 stimulation by 24 h. Analysis of *Runx2* mRNA expression was conducted after 48 h of treatment by rhBMP-2.

DOI: 10.1021/acsbiomaterials.5b00294
ACS Biomater. Sci. Eng. XXXX, XXX, XXX−XXX

against *Runx2* by NG25, NG50, and NG100 carriers produced mRNA knockdown of 55.1 ± 12.3%, 41.7 ± 13.4% and 42.8 ± 19.6%, respectively. Results indicated that *Runx2* siRNA delivery may also produce reductions in *Osx* mRNA expression (Figure 2B). Treatments delivered at NG1, NG5, and NG10 produced reductions in *Osx* mRNA expression of 56.1 ± 12.5% (p = 0.001), 56.3 ± 13.2% (p = 0.001), and 44.7 ± 15.0% (p = 0.005), respectively. In contrast, *Runx2* treatments at NG25, NG50, and NG100 resulted in *Osx* knockdown of 22.8 ± 16.9% (0.093), 9.6 ± 26% (0.526), and 23.0 ± 18.8% (p = 0.099), respectively. On the basis of target mRNA knockdown, the peak range of siRNA delivery by nanogel NSP was determined to be at NSP:siRNA ratios ranging from 1:1 to 10:1.

Assessment of siRNA dosing was conducted to determine the minimum efficacious dose required for target gene silencing (Figure 3). Results suggested that siRNA doses between 5 and 30 pmol produced significant reductions in *Runx2* mRNA expression in osteoblast cultures (Figure 3A). Doses of 20 and 30 pmol elicited statistically comparable reductions of *Runx2* gene expression caBMPR1A^{Q233D} osteoblast cultures receiving no rhBMP-2 treatment. Gene silencing by 5 and 10 pmol siRNA doses produced 59.3 ± 12.4% (p = 0.002) and 61.2 ± 10.7% (p = 0.002) reductions in *Runx2* mRNA levels, though 20 and 30 pmol doses resulted in 80.35 ± 12.9% (p < 0.001) and 84.1 ± 8.2% (p < 0.001) reductions. Secondary differences among treatment cohorts were examined by probing *Osx* gene expression (Figure 3B). Thirty picomole doses of siRNA reduced *Osx* expression by 51.6 ± 13.95% (p = 0.002), whereas doses of 5, 10, and 20 pmol reduced *Osx* mRNA expression by 13.4 ± 23.1% (p = 0.352), 42.8 ± 13.24% (p = 0.006), and 42.4 ± 15.8% (p = 0.006), respectively.

A comparison of *Runx2* siRNA delivery with control (i.e., scrambled) siRNAs was conducted to determine if the gene silencing capabilities of nanogel NSP-based RNAi therapeutics were sequence specific (Figure 4A). Results indicated that control siRNAs delivered by nanogel NSP had no significant effect on *Runx2* expression (1.4 ± 26.0% knockdown, p = 0.921), while *Runx2* siRNA delivery at NG1 demonstrated results consistent with previous studies (67.2 ± 7.9% knockdown, p < 0.001). Notably, *Runx2* siRNAs delivered without a carrier also failed to significantly impact *Runx2* expression (13.6 ± 19.7% knockdown, p = 0.290), further validating the necessity of nanogel NSPs in the development of RNAi therapeutics. It is concluded that the target gene silencing demonstrated with nanogel NSPs is dependent on both siRNA sequences and on nanogel-mediated siRNA delivery.

Subsequent to the efficacy and validation of gene silencing against *Runx2*, we investigated a combinatorial RNAi approach to silencing both *Runx2* and *Osx*. However, efficient silencing of *Runx2* and *Osx* gene expression in succession requires that the delivery of siRNAs be adjusted to target gene expression profiles. To formulate efficient siRNA delivery patterns against both genes, the effects of temporal variations in siRNA delivery against each target were assessed (Figure 4B–D). The relative expression profiles of *Runx2* and *Osx* have been reported to peak within 72 h of BMP stimulation.[38] Within this 72 h window, *Runx2* expression precedes that of *Osx* based on studies detecting *Runx2* expression in *Osx* knockout mice.[25,39] Consequently, it is expected that *Runx2* siRNAs must be delivered earlier than *Osx* in order to achieve maximal silencing of each gene. Beginning with *Runx2*, delivery times from 30 h prior to rhBMP-2 delivery (denoted "−30 h") up to simultaneous delivery with rhBMP-2 (denoted "0 h") were

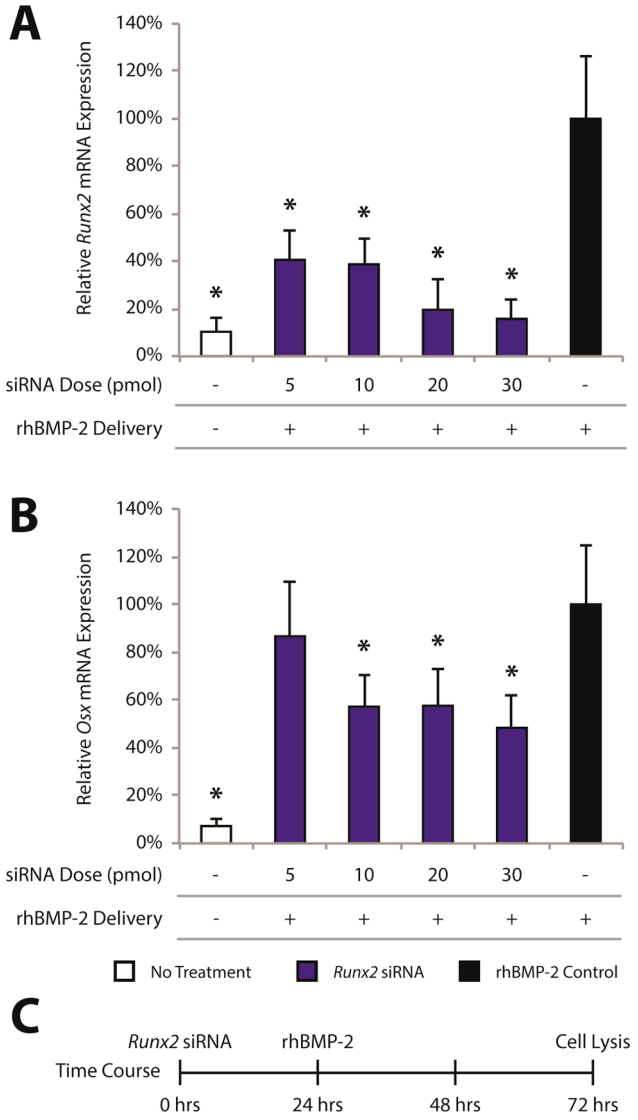

Figure 3. Analysis of siRNA dosing effects on target gene knockdown. (A) Nanogel-siRNA dosing assessment by delivery of *Runx2* siRNAs to caBMPR1A^{Q233D} osteoblasts. siRNA doses of 20 and 30 pmol, corresponding to 20 and 30 nM, produced significant reductions in *Runx2* mRNA consistent with caBMPR1A osteoblasts receiving no rhBMP-2 treatment. (B) Secondary gene silencing effects of *Runx2* siRNA dosing on *Osx* gene expression. Thirty picomole doses were deemed to be significantly different from caBMPR1A cells receiving no RNAi therapeutic; however, no statistical differences in *Osx* gene expression existed among 10, 20, and 30 pmol siRNA doses (p < 0.05). Data reported as means (n = 6) + standard deviations. Statistically significant differences are indicated by asterisks. (C) Schematic of experimental time course. siRNA delivery against *Runx2* preceded rhBMP-2 stimulation by 24 h. Analysis of *Runx2* mRNA expression was conducted after 48 h of treatment by rhBMP-2.

investigated (Figure 4B). At 24 h after rhBMP-2 stimulation, nanogel NSPs produced significant *Runx2* mRNA knockdown when *Runx2* siRNAs were delivered between −30 h and −6 h. SiRNA delivery at 0 h produced 28.9 ± 13.4% knockdown of *Runx2* expression (p = 0.051); in the context of previous *Runx2* knockdown results (Figures 2 and 3), this is a strong indicator that delivery of *Runx2* siRNA by nanogel NSP must occur prior to the BMP trigger. Peak *Runx2* silencing occurred with siRNA delivery 24 h prior to rhBMP-2, which resulted in 84.1 ± 8.9% knockdown (p < 0.001). *Runx2* knockdown at −30, −18, −12,

DOI: 10.1021/acsbiomaterials.5b00294
ACS Biomater. Sci. Eng. XXXX, XXX, XXX−XXX

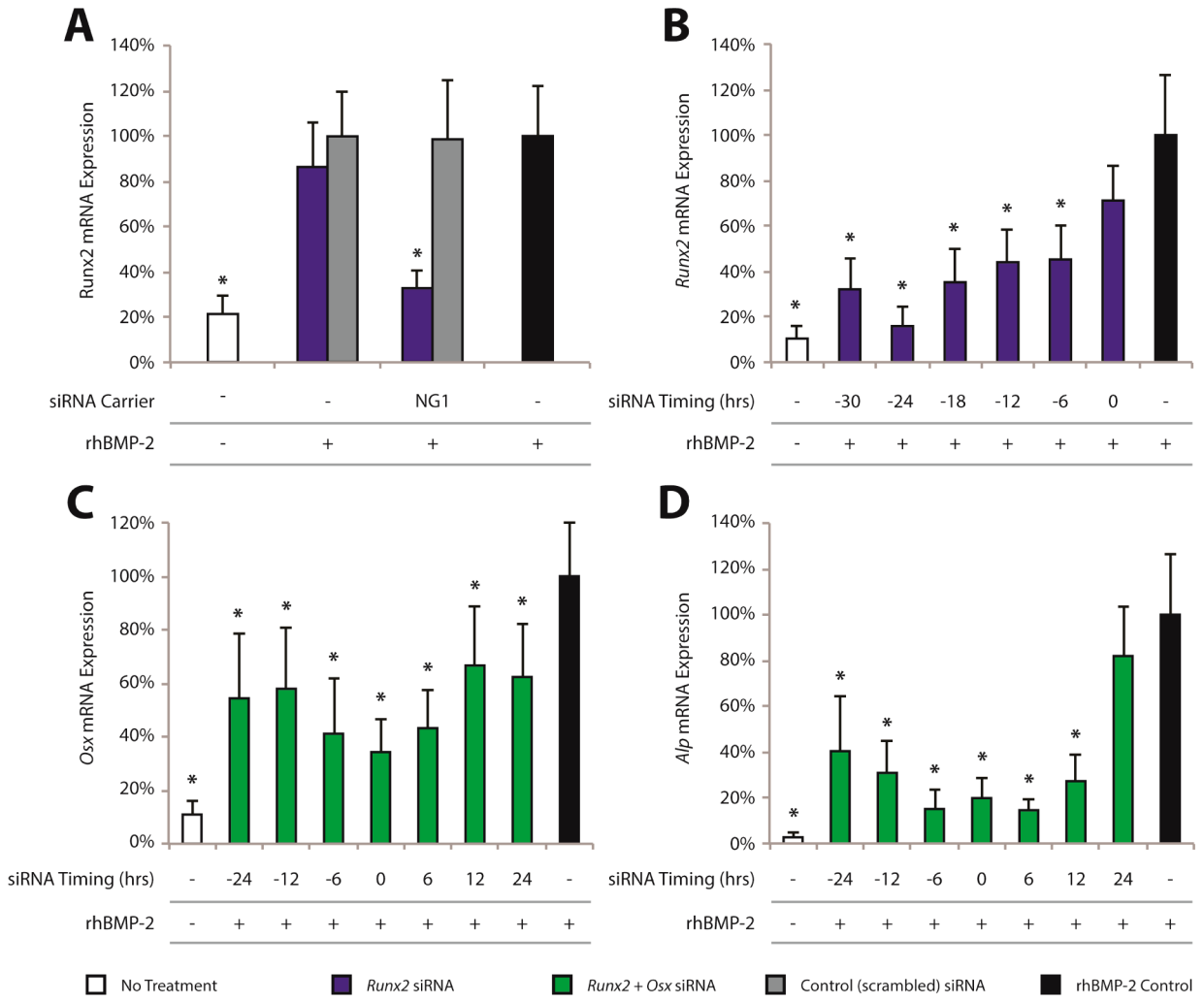

Figure 4. (A) Delivery of scrambled siRNA sequences by nanogel NSP to caBMPR1A^{Q233D} osteoblasts stimulated by rhBMP-2 had no significant effect on *Runx2* gene expression. *Runx2* siRNA delivery time course was consistent with Figures 2C and 3C. Delivery of *Runx2* siRNAs by nanogel elicited significant gene knockdown effects that were consistent with prior results ($p < 0.05$). Delivery of siRNAs (both *Runx2* and scrambled) without a nanogel carrier did not produce a silencing effect on *Runx2*. (B) Calibration of RNAi treatment timing against *Runx2* gene expression. RNAi treatments against *Runx2* were delivered at various times, ranging from 30 h prior to rhBMP-2 (−30) to simultaneous delivery (0). Though all treatments between −24 and −6 h produced statistically significant reductions in *Runx2* mRNA expression, delivery of treatments at −24 h elicited maximal gene silencing effects. (C, D) Calibration of *Osx* siRNA delivery timing against *Osx (C)* and *Alp (D)* gene expression. Delivery of *Osx* RNAi treatments between −6 and +6 h (in addition to *Runx2* siRNA delivery at −24) produced maximal gene silencing effects on *Osx* gene expression. This trend persisted when assessing *Alp* gene expression following the delivery of both *Runx2* and *Osx* siRNAs. All siRNAs delivered at 30 nM doses. Data reported as means ($n = 6$) + standard deviations; statistical significance indicated at $p < 0.05$.

and −6 h was 67.9 ± 13.4% ($p < 0.001$), 64.8 ± 14.5% ($p < 0.001$), 56.0 ± 14.5% ($p = 0.002$), and 54.8 ± 15.1% ($p = 0.002$), respectively. Though there no differences among treatments between −30 and −6 h, RNAi treatments delivered at −24 h were comparable to cells untreated with rhBMP-2 ($p = 0.2165$) (Figure 4B).

Following this calibration of siRNA delivery timing against *Runx2*, the timing of *Osx* siRNA delivery for peak silencing of *Osx* gene expression was investigated in increments of 6 h, ranging from −24 to +24 h, relative to rhBMP-2 delivery. *Osx* siRNA was delivered following an initial delivery of *Runx2* siRNA at −24 h. This was dictated by our logic to attack *Runx2* and *Osx* expression in combination. Analysis of *Osx* (Figure 4C) gene expression determined that *Osx* siRNA delivery during the temporal window ranging from −6 and +6 h demonstrated significant target mRNA knockdown, achieving 58.9 ± 20.7%, 65.7 ± 12.4%, and 56.7 ± 14.4% knockdown, respectively ($p < 0.001$). Though siRNA delivery at −24, −12, + 12, and +24 h also produced significant *Osx* knockdown ($p < 0.05$), significant differences existed between the 0 h treatment, and treatments at +12 and +24 ($p < 0.05$). Secondary differences among temporal groups were investigated by simultaneously probing alkaline phosphatase (*Alp*) gene expression (Figure 4D). Assessment of *Alp* gene expression determined that the peak knockdown of 85.5 ± 4.4% was produced by *Osx* siRNA delivery at +6 h relative to rhBMP-2 ($p < 0.001$). This knockdown was consistent with *Osx* siRNA delivery at −6 and 0 h, which produced *Alp* mRNA reductions of 84.9 ± 8.2% and 80.2 ± 9.1%, respectively ($p < 0.001$). Combined *Osx* and *Alp* knockdown suggests that the optimal window for delivery of *Osx* siRNAs is within 6 h of rhBMP-2 delivery. The temporal profiling of these nanogel NSP-mediated siRNA therapeutics supports a *Runx2* targeting time 24 h prior to rhBMP-2 delivery (−24 h) and an *Osx* targeting

DOI: 10.1021/acsbiomaterials.5b00294
ACS Biomater. Sci. Eng. XXXX, XXX, XXX−XXX

time at the same time as the rhBMP-2 trigger (0 h). This approach was extended to produce a repeatable 48-h cycle of RNAi treatments with repeated *Runx2* and *Osx* siRNA delivery by nanogel NSPs with 24-h intervals.

Reductions in *Alp* gene expression after nanogel-mediated delivery of siRNAs against *Runx2* and *Osx* indicated the ability to modulate expression of downstream osteoblast differentiation markers by RNAi. During osteogenic differentiation, alkaline phosphatase, in particular, plays an important role in the deposition of hydroxyapatite through the conversion of pyrophosphate groups into phosphate ions. Though we previously probed *Alp* expression 48 h into the osteogenic differentiation process (Figure 4D), peak expression of *Alp* is known to occur between 7 and 14 days in an osteogenic cell culture environment.[40] Enzymatic analyses of ALP protein levels after 4, 7, and 14 days in culture were conducted to quantify downstream gene silencing (Figure 5A–C). Nanogel-mediated siRNA delivery was exploited at 1:1 (NG1) and 5:1(NG5) nanogel:siRNA ratios, which were down-selected from qRT-PCR studies based on consistent target gene knockdown capabilities. RNAi treatments against *Runx2* and *Osx* were delivered in repeated 48-h treatment cycles that were carried out to 4, 7, and 14 days (Figure 5D). Results demonstrated that nanogel NSPs delivering *Runx2* and *Osx* siRNAs at NG1 and NG5 ratios significantly reduced ALP activity at all experimental temporal periods ($p < 0.001$). However, despite reduced ALP activity in comparison to rhBMP-2 control groups, significant differences ($p < 0.001$ at 4, 7, and 14 days) persisted between polyplex treated groups and control cells that received no rhBMP-2 trigger. It may be concluded that while significant reductions in ALP activity were observed, full suppression of ALP activity may not be achieved by solely targeting *Runx2* and *Osx*. Alternatively, additional (unimpeded) pathways stimulating *Alp* expression may be responsible. RNAi targeting of the *Alp* gene was investigated by simultaneous delivery of *Alp* siRNA with *Osx* siRNA treatments (Figure 6). Treatment cohorts were expanded to include siRNA delivery by NG10 and Lipofectamine RNAiMAX (denoted LRM), a commercially available lipid-based siRNA delivery reagent. The inclusion of *Alp* siRNAs in the treatment course produced marked reductions in ALP activity during 4-, and 14-day cultures. At 4 days in culture, ALP activity in all RNAi-treated cultures was reduced to levels consistent with caBMPR1A osteoblasts that did not receive rhBMP-2 triggers ($p > 0.05$). Among treated groups, cultures treated with NG1, NG5, and LRM carriers exhibited lower ALP levels than those treated by NG10 carriers (all $p < 0.040$). The indication from this result is that at early levels of ALP upregulation, the strength of RNAi treatments was sufficient to completely abrogate expression levels; further, the efficacy of siRNA delivered by NG10 carriers lagged behind NG1, NG5 and LRM. At 7 days, significant reductions in ALP activity were elicited by NG1, NG5, and LRM treatments (all $p < 0.02$), though these treatments did not completely reduce ALP activity to baseline levels (all $p < 0.002$); there were no significant differences among NG1, NG5, and LRM treatments ($p > 0.05$). NG10 RNAi treatments did not produce significant reductions in ALP activity after 7 days in culture ($p > 0.05$). At 14 days, all RNAi treatments caused significant reduction in ALP activity ($p < 0.001$), with NG1 and NG5 RNAi treatments producing the greatest reductions in ALP activity. NG10 treatments were outperformed by both NG1 and NG5 treatments (both $p < 0.001$). Comparisons to Lipofectamine

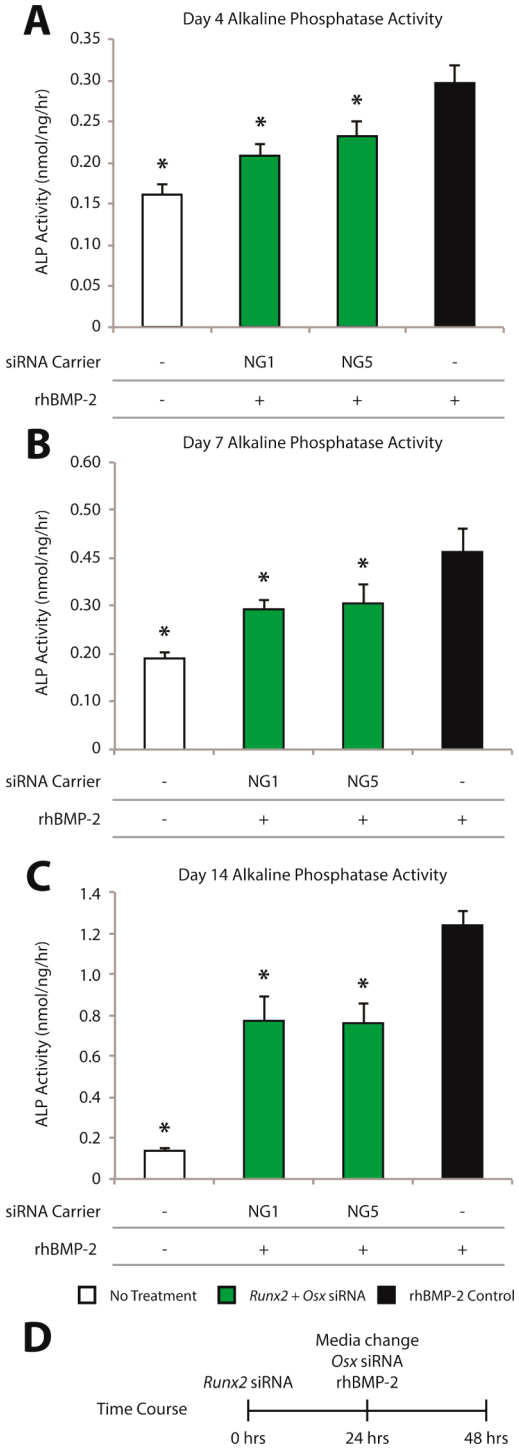

Figure 5. Quantification of alkaline phosphatase (ALP) activity after (A) 4, (B) 7, and (C) 14 days in culture. (D) Osteoblastic differentiation was stimulated by rhBMP-2 delivery every 48 h, along with repeated RNAi treatments against *Runx2* and *Osx*. Significant reductions in ALP activity were produced by nanogel 1:1 (NG1) and 5:1 (NG5) treatments at all three temporal periods. SiRNAs delivered at 30 nM final concentrations. Data reported as means ($n = 6$) + standard deviations; statistical significance indicated at $p < 0.05$ relative to cell cultures receiving rhBMP-2 treatments alone (black bars).

were favorable for nanogel NSPs; NG1 and NG5 treatments both produced significant reductions in ALP activity in relation to Lipofectamine (both $p < 0.001$). At both day 7 and 14 of this study, though reductions in ALP activity in RNAi-treated

DOI: 10.1021/acsbiomaterials.5b00294
ACS Biomater. Sci. Eng. XXXX, XXX, XXX–XXX

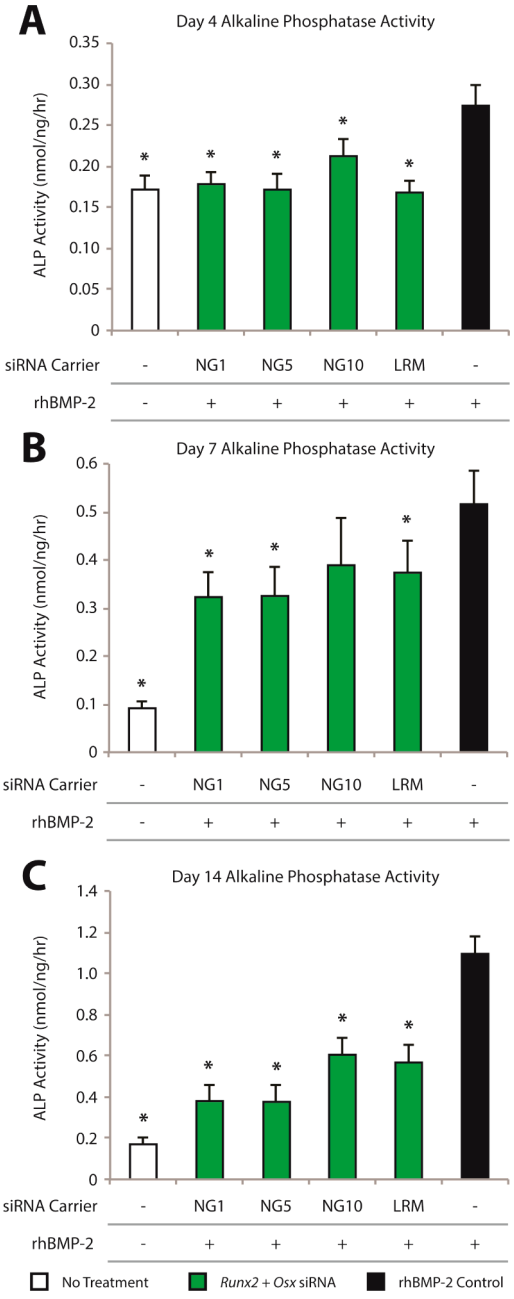

Figure 6. Quantification of ALP activity after (A) 4, (B) 7, and (C) 14 days in culture after delivery of RNAi treatments against *Runx2*, *Osx*, and *Alp*. (D) siRNAs against *Alp* were delivered simultaneously with *Osx* RNAi treatments to caBMPR1A^{Q233D} osteoblasts. Significant reductions in ALP activity were produced at all three experimental end points by nanogel 1:1 (NG1) and 5:1 (NG5) ratios. ALP knockdown by NG1 and NG5 treatments were comparable to treatments delivered by Lipofectamine RNAiMAX (LRM). NG10 treatments induced significant reductions in ALP activity, though knockdown efficiency was consistently lower than NG1 and NG5 treatments ($p < 0.05$). SiRNA delivered at 30 nM final concentrations. Data reported as means ($n = 8$) + standard deviations; statistical significance indicated at $p < 0.05$ with respect to cell cultures receiving rhBMP-2 treatments alone (black bars).

groups were significant, they were not reduced to levels consistent with caBMPR1A osteoblasts receiving no rhBMP-2 treatment (all $p < 0.001$). As such, despite notable reductions in ALP activity by efficient polymeric delivery of siRNAs against *Runx2*, *Osx*, and *Alp1*, the challenge of full suppression of ALP activity persists. However, even incomplete knockdown effects may produce a significant impact on osteoblastic differentiation; thus, we investigated the deposition of mineralization in rhBMP-2-treated cultures receiving RNAi treatments.

An assessment of mineralization after 28 days in culture was accomplished using von Kossa and Alizarin Red S staining (Figure 7). Delivery of *Runx2* and *Osx* siRNAs by nanogel NSPs at NG1 and NG5 ratios resulted in reduced von Kossa staining intensity, indicating a decrease in mineralization to levels comparable to osteoblasts that did not receive a BMP trigger (Figure 7A). Nanogel RNAi treatments at 10:1 indicated staining consistent with caQ233D osteoblasts receiving rhBMP-2 treatments. Lipofectamine RNAiMAX was again evaluated as a reference material, delivering siRNAs against both *Runx2* and *Osx*. A similar reduction of mineralization was noted, with staining levels consistent with untreated caQ233D osteoblasts. Results were confirmed by independent staining with Alizarin Red S (Figure 7B). Cultures receiving NG1 and NG5 RNAi treatments produced staining intensities comparable to RNAiMAX and untreated cell cohorts. This reduction is evident despite incomplete suppression of ALP activity, suggesting that hydroxyapatite deposition may be impacted by even modest reductions in ALP activity. Further, notable reductions in mineralization are obtained when delivering siRNAs against *Runx2* and *Osx* using nanogel NSPs at NG1 and NG5. Overall, the efficacy of nanogel NSPs was comparable to the commercially available transfection reagent, Lipofectamine RNAiMAX.

Quantification of mineralization processes was performed through execution of the OsteoImage assay after 7, 14, 21, and 28 days in culture (Figure 8). RNAi treatments against *Runx2* and *Osx* produced consistent reductions in hydroxyapatite deposition regardless of the siRNA carrier ($p < 0.05$). Though all treatments demonstrated efficacy, NG1, NG5, and LRM produced significantly greater knockdown than NG10 treatments (all $p < 0.01$). It is notable that over 14, 21, and 28 day time points, no RNAi treatment was able to inhibit HA deposition to levels comparable to osteoblasts that did not receive rhBMP-2 triggers (all $p < 0.01$). Despite this inability to completely abrogate osteogenic differentiation in caBMPR1A osteoblasts, nanogel NSPs demonstrate the potential for efficient gene silencing and knockdown (comparable to Lipofectamine RNAiMAX) without any discernible cytotoxic effects.

DISCUSSION

The nanogel NSPs employed here for gene knockdown are the culmination of exploring multiple strategies for overcoming the barriers that have traditionally limited the efficacy of polymeric siRNA delivery platforms. Initial assessments of nanogel efficacy were conducted in proof-of-concept insect and mammalian cell lines.[19,20] Trauma-induced HO and FOP provide testing environments in which nanogel NSPs can be further optimized for the development of RNAi treatments. The reduced target mRNA expression produced by nanogel-mediated siRNA delivery are strong indicators that molecular-level features to protect siRNAs from degradation, escape from endosomal degradation pathways, and release siRNA in cytoplasmic environments demonstrate utility in cellular environments.[19]

We report the ability to knockdown key osteoblast differentiation markers by RNAi therapeutics in caBM-

DOI: 10.1021/acsbiomaterials.5b00294
ACS Biomater. Sci. Eng. XXXX, XXX, XXX−XXX

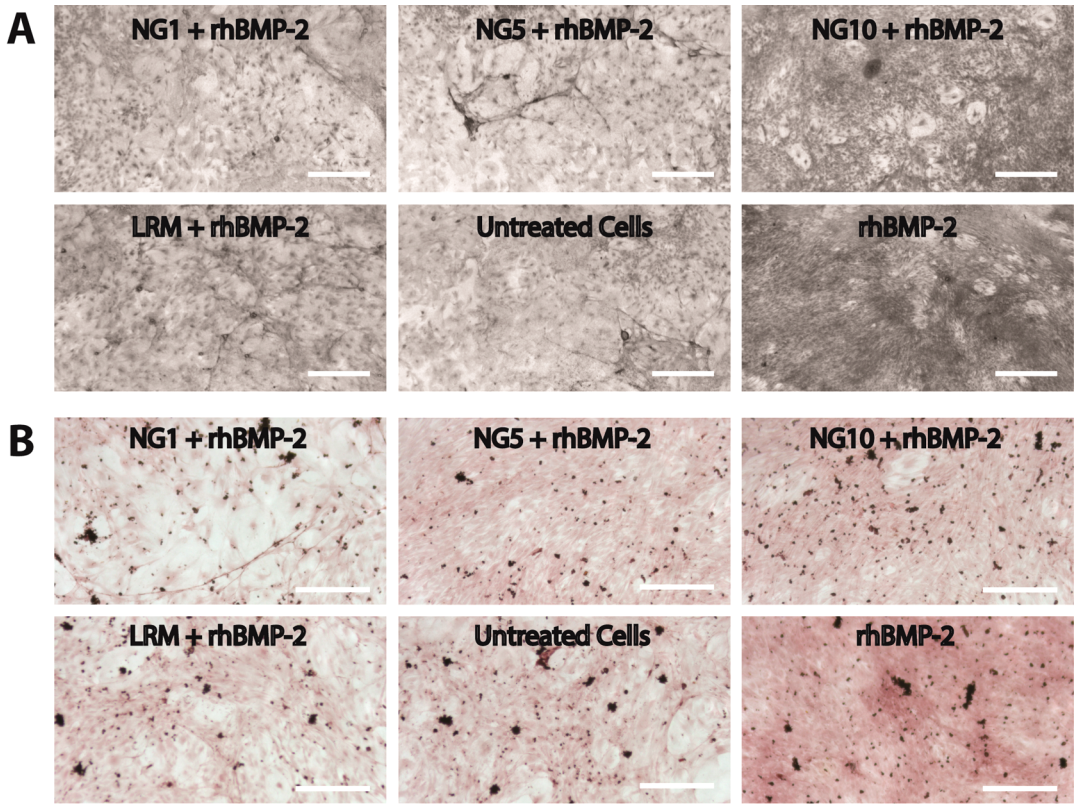

Figure 7. Mineralization studies in caBMPR1A^{Q233D} osteoblasts via (A) von Kossa and (B) Alizarin Red S staining after 28 days. Results indicated substantial reductions in staining intensity in cultures receiving nanogel 1:1 (NG1) and 5:1 (NG5) RNAi treatments against the effects of rhBMP-2. NG1 and NG5 treatments inhibited mineralization consistent with LipofectamineRNAiMAX (LRM) and caBMPR1A^{Q233D} osteoblasts receiving no treatments (bottom left). Cultures receiving NG10 RNAi treatments reflected reduced knockdown efficiency. Results were consistent across both staining methods. SiRNA delivered at 30 nM final concentrations. (A) Scale bar, 1 mm. (B) Scale bar, 500 μm.

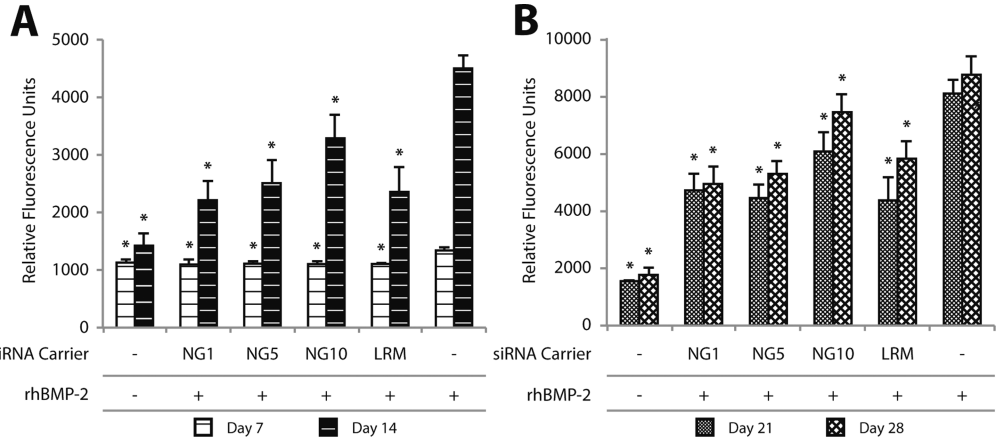

Figure 8. OsteoImage-based quantification of hydroxyapatite (HA) deposition in caBMPR1A^{Q233D} osteoblasts at (A) 7 and 14 days, and (B) 21 and 28 days. All RNAi treatments (delivered to 30 nM final siRNA concentration) inhibited HA deposition significantly, though the degree of suppression varied. NG1 and NG5 treatments both demonstrated reduction in HA deposition similar to Lipofectamine RNAiMAX (LRM). NG10 showed some reduction in HA deposition, though suppression was significantly reduced in comparison to NG1, NG5, and LRM treatments ($p > 0.05$). Despite significant reductions, no treatment reduced HA deposition to baseline levels, indicated by untreated caBMPR1A^{Q233D} osteoblasts ($p < 0.01$). Data reported as means ($n = 4$) + standard deviations; statistical significance indicated at $p < 0.05$.

PR1A^{Q233D} primary osteoblasts stimulated with rhBMP-2. Peak mRNA knockdown ranged from 60 to 80% by nanogel:siRNA ratios from 1:1 to 5:1. However, despite this knockdown, we deduced that mRNA translation of target genes was still occurring at levels greater than the baseline. Despite RNAi attack, osteoblast markers were still being produced after stimulation by rhBMP-2. We also present evidence that full suppression of osteoblast markers is not necessary to impede hydroxyapatite deposition in cell cultures. This knockdown attained by nanogel NSPs delivering siRNAs against *Runx2* and *Osx* is consistent with the best available commercial siRNA delivery vehicles, including Lipofectamine RNAiMAX. Further, there are no apparent cytotoxic effects associated with cationic nanogel NSPs. In comparison to other polymeric approaches

DOI: 10.1021/acsbiomaterials.5b00294
ACS Biomater. Sci. Eng. XXXX, XXX, XXX−XXX

for siRNA delivery, the vast majority of these contemporary options require low-serum or no-serum conditions to maintain siRNA integrity and binding. With this nanogel NSP, we demonstrate significant knockdown of a target gene in cell cultures supplemented with 10% serum to better simulate the challenges associated with in vivo siRNA delivery. Our results here suggest that we have produced advances in the knockdown capabilities of polymeric siRNA delivery platforms.

This is further supported by evidence that even modest reductions in *Runx2* can produce biological consequences. *Runx2* heterozygous humans, for example, consistently develop bone abnormalities such as cleidocranial dysplasia.[41] Thus, even an incomplete suppression of *RUNX2* and *OSX* expression in HO patients may form the basis of a viable localized HO prophylaxis.

Downstream analysis of knockdown revealed reduced alkaline phosphatase (ALP) activity in response to nanogel 1:1 and 5:1 RNAi treatments against *Runx2* and *Osx*. The reduction of alkaline phosphatase is a significant milestone in prevention of osteogenic differentiation, as it plays an important role in calcification processes by hydrolyzing pyrophosphates into phosphates that fuel mineralization processes along with Ca^{2+} ions. Alkaline phosphatase, while being crucial for hydroxyapatite deposition, has not been linked directly to *Runx2* gene expression.[42] Rather, ALP expression is typically connected to the canonical WNT signaling pathway through β-catenin. This pathway may be activated by BMP-2 via SMAD signaling proteins and/or the mitogen-activated protein kinase (MAPK) pathway.[43] However, because of BMP-induced expression of the transcription factor *Dlx5*, *Osx* and ultimately *Alp* are upregulated.[44] On the basis of this connection, it has been reported that induction of *Runx2* and *Osx* lead to significant ALP activity.[45] Thus, the inclusion of *Osx* siRNAs in this study and the subsequent reductions in ALP activity may validate the connection between the two. Additionally, the results we report here are further evidence that reduced expression of *Runx2* and *Osx* mRNAs may reduce ALP activity.[30]

Prior reports of inhibiting osteogenic differentiation and bone formation by silencing *Runx2* have employed adenoviral siRNA delivery, rather than the nonviral means we report here.[30] While adenoviral means of gene delivery typically achieve greater gene knockdown than nonviral alternatives, potential safety concerns have tempered enthusiasm for their use in the clinic. Further, challenges in scale-up of viral vectors have also limited their utility for large-scale production. To our knowledge, there are currently no clinical RNAi programs that employ viral delivery of siRNA. At this time, lipid-based formulations are the most advanced nonviral siRNA carrier, though their limitations (dose-dependent toxicity, rapid clearance from circulation) necessitate the exploration of alternatives.[46,47]

ATRP has enabled the production of nanogel NSPs with varying charge densities, polymer composition, and functionalities. They can be synthesized in bulk emulsification reactions that can be scaled up for mass production. Nanogels also exhibit a narrow monomodal size distribution and consistent siRNA loading characteristics among batches.[19] Further, we have demonstrated that nanogel NSPs consistently produce target gene knockdown comparable to the commercial standard, Lipofectamine RNAiMAX, though without any noted cytotoxic effects.. Nanogel NSPs may provide a substantial improvement over viral vectors and commercial lipid-based formulations with regards to safety without significantly impacting knockdown capabilities.

CONCLUSIONS

Here, nanogel NSPs were employed for the delivery of siRNAs against *Runx2* and *Osx* in primary osteoblasts isolated a transgenic mouse model for HO. Key delivery parameters for RNAi therapeutics against FOP were calibrated, including NSP:siRNA ratios, siRNA doses and the relative timing of RNAi therapeutics against *Runx2* and *Osx* gene expression. Gene knockdown capabilities were established, and produced sequence-specific gene knockdown effects on *Runx2* and *Osx*. Treatment cycles were formulated based on a staggered, coordinated RNAi attack on *Runx2* and *Osx*; outcomes suggested silencing of downstream osteoblast differentiation marker ALP after 4, 7, and 14 days in culture. RNAi therapeutics produced a significant reduction in hydroxyapatite formation in vitro, though HA deposition remained above baseline levels. Significant challenges persist in the production of treatments that will fully abrogate rogue bone formation in HO patients. However, because the anatomical location of heterotopic bone formation is highly correlated to the site of a traumatic insult (e.g., an amputation/arthroplasty site, or a flare up in FOP patients), a prophylaxis to be administered at an injury site has clinical merit. Here, study data underscored the compelling therapeutic opportunity to target *Runx2* and *Osx* in the BMP signaling pathway to inhibit osteogenic differentiation. The targeting of additional mid- and late-stage osteoblast markers of alkaline phosphatase, osteocalcin, osteonectin, and bone sialoprotein may improve the potency of RNAi therapeutics for prevention of osteogenic differentiation. Elucidation and identification of additional targets may result in a more comprehensive therapeutic portfolio that will prevent osteoblast lineage progression and subsequent heterotopic bone formation in the clinic.

ASSOCIATED CONTENT

Supporting Information

The Supporting Information is available free of charge on the ACS Publications website at DOI: 10.1021/acsbiomaterials.5b00294.

Characterization of caBMPR1A primary osteoblasts with a Q233D mutation (Figure S1), and a schematic of nanogel NSP synthesis (Figure S2) (PDF)

AUTHOR INFORMATION

Corresponding Author

*E-mail: jhollinge@andrew.cmu.edu. Phone: 412-559-5536.

Present Addresses

‡A.R.S. is currently at John A Paulson School of Engineering and Applied Sciences, Harvard University, 29 Oxford Street, Cambridge, Massachusetts 02138, United States

#S.E.A. is currently at Allegheny General Hospital South Tower, Room 1179, 320 E. North Avenue, Pittsburgh, Pennsylvania 15212, United States

Author Contributions

Research was designed by A.R.S., S.E.A, H.P, K.M., Y.M., and J.O.H; materials were prepared by A.R.S., M.C.M., S.E.A., H.P., and Y.M.; experiments were performed by A.R.S., M.C.M., M.K., H.P., and Y.M.; data were analyzed by A.R.S., H.P., and Y.M.; manuscript was written by A.R.S., M.C.M., S.E.A., H.P.,

DOI: 10.1021/acsbiomaterials.5b00294
ACS Biomater. Sci. Eng. XXXX, XXX, XXX−XXX

K.M., Y.M., and J.O.H. All authors have given approval to the final version of the manuscript.

Funding

The authors gratefully acknowledge DMR-1501324 and Department of Defense Grant W81XWH1120073, which was awarded by the Defense Medical Research and Development Program, for funding. Y.M. and K.M. are supported by the National Institutes of Health (R01DE020843).

Notes

The authors declare no competing financial interest.

■ ACKNOWLEDGMENTS

The authors thank Dr. Kenichi Yamamura for providing *P0-Cre* mice, *C57BL/6J-Tg(P0-Cre)94Imeg* (ID 148) and Dr. Takeshi Imamura for providing *caBmpr1a* Q233D constructs.

■ ABBREVIATIONS

siRNA, short interfering ribonucleic acid
NSP, nanostructured polymer
RNAi, ribonucleic acid interference
DMAEMA, dimethylaminoethyl methacrylate
PEG, polyethylene glycol
ATRP, atom transfer radical polymerization
Runx2, Runt-related transcription factor 2
Osx, Osterix
BMP, bone morphogenetic protein
BMPR1A, BMP receptor 1A
ACVR1/ALK2, Activin A receptor, type 1/Activin-like kinase 2
HO, heterotopic ossification
FOP, fibrodysplasia ossificans progressiva
NSAIDS, nonsteroidal anti-inflammatory drugs
ALP, alkaline phosphatase

■ REFERENCES

(1) Garland, D. E. A clinical perspective on common forms of acquired heterotopic ossification. *Clin. Orthop. Relat. Res.* **1991**, *263*, 13−29.
(2) Parkinson, J. R.; Evarts, C. M.; Hubbard, L. F. Radiation therapy in the prevention of heterotopic ossification after total hip arthroplasty. *Hip* **1982**, 211−227.
(3) Tsionos, I.; Leclercq, C.; Rochet, J. M. Heterotopic ossification of the elbow in patients with burns. Results after early excision. *J. Bone Jt. Surg., Br. Vol.* **2004**, *86* (3), 396−403.
(4) Forsberg, J. A.; Pepek, J. M.; Wagner, S.; Wilson, K.; Flint, J.; Andersen, R. C.; Tadaki, D.; Gage, F. A.; Stojadinovic, A.; Elster, E. A. Heterotopic ossification in high-energy wartime extremity injuries: prevalence and risk factors. *Journal of bone and joint surgery. American volume* **2009**, *91* (5), 1084−91.
(5) Connor, J. M.; Evans, D. A. Fibrodysplasia ossificans progressiva. The clinical features and natural history of 34 patients. *J. Bone. Joint Surg. Br.* **1982**, *64*, 76−83.
(6) Kaplan, F. S.; Zasloff, M. A.; Kitterman, J. A.; Shore, E. M.; Hong, C. C.; Rocke, D. M. Early mortality and cardiorespiratory failure in patients with fibrodysplasia ossificans progressiva. *J. Bone Jt. Surg. Am.* **2010**, *92* (3), 686−691.
(7) Shrivats, A. R.; Alvarez, P.; Schutte, L.; Hollinger, J. O., Bone Regeneration. In *Principles of Tissue Engineering*, 4th ed.; Lanza, R., Langer, R., Vacanti, J., Eds.; Elsevier: San Diego, 2014; pp 1201−1221.
(8) Kan, L.; Kessler, J. A. Animal models of typical heterotopic ossification. *J. Biomed. Biotechnol.* **2011**, *2011*, 309287.
(9) Shore, E. M.; Xu, M.; Feldman, G. J.; Fenstermacher, D. A.; Cho, T. J.; Choi, I. H.; Connor, J. M.; Delai, P.; Glaser, D. L.; LeMerrer, M.; Morhart, R.; Rogers, J. G.; Smith, R.; Triffitt, J. T.; Urtizberea, J. A.; Zasloff, M.; Brown, M. A.; Kaplan, F. S. A recurrent mutation in the BMP type I receptor ACVR1 causes inherited and sporadic fibrodysplasia ossificans progressiva. *Nat. Genet.* **2006**, *38* (5), 525−7.
(10) Gannon, F. H.; Kaplan, F. S.; Olmsted, E.; Finkel, G. C.; Zasloff, M. A.; Shore, E. Bone morphogenetic protein 2/4 in early fibromatous lesions of fibrodysplasia ossificans progressiva. *Hum. Pathol.* **1997**, *28* (3), 339−43.
(11) Whelton, A. Nephrotoxicity of nonsteroidal anti-inflammatory drugs: physiologic foundations and clinical implications. *Am. J. Med.* **1999**, *106* (5B), 13S−24S.
(12) Chao, S. T.; Joyce, M. J.; Suh, J. H. Treatment of heterotopic ossification. *Orthopedics* **2007**, *30* (6), 457−464.
(13) Healy, W. L.; Lo, T. C.; Covall, D. J.; Pfeifer, B. A.; Wasilewski, S. A. Single-dose radiation therapy for prevention of heterotopic ossification after total hip arthroplasty. *J. Arthroplasty* **1990**, *5* (4), 369−375.
(14) Smith, R. Fibrodysplasia (myositis) ossificans progressiva. Clinical lessons from a rare disease. *Clin. Orthop. Relat. Res.* **1998**, *346*, 7−14.
(15) Wang, J.; Lu, Z.; Wientjes, M. G.; Au, J. L. Delivery of siRNA therapeutics: barriers and carriers. *AAPS J.* **2010**, *12* (4), 492−503.
(16) Matyjaszewski, K. Atom Transfer Radical Polymerization (ATRP): Current Status and Future Perspectives. *Macromolecules* **2012**, *45* (10), 4015−4039.
(17) Matyjaszewski, K.; Xia, J. Atom transfer radical polymerization. *Chem. Rev.* **2001**, *101* (9), 2921−90.
(18) Matyjaszewski, K.; Tsarevsky, N. V. Macromolecular engineering by atom transfer radical polymerization. *J. Am. Chem. Soc.* **2014**, *136* (18), 6513−33.
(19) Averick, S. E.; Paredes, E.; Irastorza, A.; Shrivats, A. R.; Srinivasan, A.; Siegwart, D. J.; Magenau, A. J.; Cho, H. Y.; Hsu, E.; Averick, A. A.; Kim, J.; Liu, S.; Hollinger, J. O.; Das, S. R.; Matyjaszewski, K. Preparation of cationic nanogels for nucleic acid delivery. *Biomacromolecules* **2012**, *13* (11), 3445−9.
(20) Hsu, E. W.; Liu, S.; Shrivats, A. R.; Watt, A.; McBride, S.; Averick, S. E.; Cho, H. Y.; Matyjaszewski, K.; Hollinger, J. O. Cationic Nanostructured Polymers for siRNA Delivery in Murine Calvarial Pre-Osteoblasts. *J. Biomed. Nanotechnol.* **2014**, *10* (6), 1130−1136.
(21) Shrivats, A. R.; Hsu, E.; Averick, S.; Klimak, M.; Watt, A. C.; DeMaio, M.; Matyjaszewski, K.; Hollinger, J. O. Cationic Nanogel-mediated Runx2 and Osterix siRNA Delivery Decreases Mineralization in MC3T3 Cells. *Clin. Orthop. Relat. Res.* **2015**, *473*, 2139.
(22) Agarwal, S.; Zhang, Y.; Maji, S.; Greiner, A. PDMAEMA based gene delivery materials. *Mater. Today* **2012**, *15* (9), 388−393.
(23) Shrivats, A. R.; Mishina, Y.; Averick, S.; Matyjaszewski, K.; Hollinger, J. O. In Vivo GFP Knockdown by Cationic Nanogel-siRNA Polyplexes. *Bioengineering* **2015**, *2* (3), 160−175.
(24) Drissi, H.; Luc, Q.; Shakoori, R.; Chuva De Sousa Lopes, S.; Choi, J. Y.; Terry, A.; Hu, M.; Jones, S.; Neil, J. C.; Lian, J. B.; Stein, J. L.; Van Wijnen, A. J.; Stein, G. S. Transcriptional autoregulation of the bone related CBFA1/RUNX2 gene. *J. Cell. Physiol.* **2000**, *184* (3), 341−50.
(25) Nishio, Y.; Dong, Y.; Paris, M.; O'Keefe, R. J.; Schwarz, E. M.; Drissi, H. Runx2-mediated regulation of the zinc finger Osterix/Sp7 gene. *Gene* **2006**, *372*, 62−70.
(26) Ryoo, H.-M.; Lee, M.-H.; Kim, Y.-J. Critical molecular switches involved in BMP-2-induced osteogenic differentiation of mesenchymal cells. *Gene* **2006**, *366* (1), 51−57.
(27) Franceschi, R. T.; Xiao, G.; Jiang, D.; Gopalakrishnan, R.; Yang, S.; Reith, E. Multiple signaling pathways converge on the Cbfa1/Runx2 transcription factor to regulate osteoblast differentiation. *Connect. Tissue Res.* **2003**, *44* (Suppl 1), 109−116.
(28) Komori, T. Runx2, a multifunctional transcription factor in skeletal development. *J. Cell. Biochem.* **2002**, *87* (1), 1−8.
(29) Nakashima, K.; Zhou, X.; Kunkel, G.; Zhang, Z.; Deng, J. M.; Behringer, R. R.; de Crombrugghe, B. The novel zinc finger-containing transcription factor osterix is required for osteoblast differentiation and bone formation. *Cell* **2002**, *108* (1), 17−29.
(30) Lin, L.; Chen, L.; Wang, H.; Wei, X.; Fu, X.; Zhang, J.; Ma, K.; Zhou, C.; Yu, C. Adenovirus-mediated transfer of siRNA against

DOI: 10.1021/acsbiomaterials.5b00294
ACS Biomater. Sci. Eng. XXXX, XXX, XXX−XXX

Runx2/Cbfa1 inhibits the formation of heterotopic ossification in animal model. *Biochem. Biophys. Res. Commun.* **2006**, *349* (2), 564−72.
(31) Mishra, S.; Vaughn, A. D.; Devore, D. I.; Roth, C. M. Delivery of siRNA silencing Runx2 using a multifunctional polymer-lipid nanoparticle inhibits osteogenesis in a cell culture model of heterotopic ossification. *Integrative biology: quantitative biosciences from nano to macro* **2012**, *4* (12), 1498−507.
(32) Kamiya, N.; Ye, L.; Kobayashi, T.; Mochida, Y.; Yamauchi, M.; Kronenberg, H. M.; Feng, J. Q.; Mishina, Y. BMP signaling negatively regulates bone mass through sclerostin by inhibiting the canonical Wnt pathway. *Development* **2008**, *135* (22), 3801−11.
(33) Komatsu, Y.; Yu, P. B.; Kamiya, N.; Pan, H.; Fukuda, T.; Scott, G. J.; Ray, M. K.; Yamamura, K.; Mishina, Y. Augmentation of Smad-dependent BMP signaling in neural crest cells causes craniosynostosis in mice. *J. Bone Miner. Res.* **2013**, *28* (6), 1422−33.
(34) Lavery, K.; Swain, P.; Falb, D.; Alaoui-Ismaili, M. H. BMP-2/4 and BMP-6/7 differentially utilize cell surface receptors to induce osteoblastic differentiation of human bone marrow-derived mesenchymal stem cells. *J. Biol. Chem.* **2008**, *283* (30), 20948−58.
(35) Yamauchi, Y.; Abe, K.; Mantani, A.; Hitoshi, Y.; Suzuki, M.; Osuzu, F.; Kuratani, S.; Yamamura, K. A novel transgenic technique that allows specific marking of the neural crest cell lineage in mice. *Dev. Biol.* **1999**, *212* (1), 191−203.
(36) Shrivats, A. R.; Hollinger, J. O., The Delivery and Evaluation of RNAi Therapeutics for Heterotopic Ossification Pathologies. In *Biomimetics and Stem Cells: Methods and Protocols*; Turksen, K., Vunjak-Novakovic, G., Eds.; SpringerLink: New York, 2013.
(37) Eliyahu, H.; Barenholz, Y.; Domb, A. J. Polymers for DNA delivery. *Molecules* **2005**, *10* (1), 34−64.
(38) Komori, T. Regulation of osteoblast differentiation by transcription factors. *J. Cell. Biochem.* **2006**, *99* (5), 1233−9.
(39) Chen, M.; Zhao, M.; Harris, S. E.; Mi, Z. Signal transduction and biological functions of bone morphogenetic proteins. *Front. Biosci., Landmark Ed.* **2004**, *9*, 349−358.
(40) Prince, M.; Banerjee, C.; Javed, A.; Green, J.; Lian, J. B.; Stein, G. S.; Bodine, P. V.; Komm, B. S. Expression and regulation of Runx2/Cbfa1 and osteoblast phenotypic markers during the growth and differentiation of human osteoblasts. *J. Cell. Biochem.* **2001**, *80* (3), 424−40.
(41) Otto, F.; Kanegane, H.; Mundlos, S. Mutations in the RUNX2 gene in patients with cleidocranial dysplasia. *Hum. Mutat.* **2002**, *19* (3), 209−16.
(42) Rawadi, G.; Vayssiere, B.; Dunn, F.; Baron, R.; Roman-Roman, S. BMP-2 controls alkaline phosphatase expression and osteoblast mineralization by a Wnt autocrine loop. *J. Bone Miner. Res.* **2003**, *18* (10), 1842−53.
(43) Bikkavilli, R. K.; Malbon, C. C. Mitogen-activated protein kinases and Wnt/beta-catenin signaling: Molecular conversations among signaling pathways. *Commun. Integr. Biol.* **2009**, *2* (1), 46−9.
(44) Ulsamer, A.; Ortuno, M. J.; Ruiz, S.; Susperregui, A. R.; Osses, N.; Rosa, J. L.; Ventura, F. BMP-2 induces Osterix expression through up-regulation of Dlx5 and its phosphorylation by p38. *J. Biol. Chem.* **2008**, *283* (7), 3816−26.
(45) Matsubara, T.; Kida, K.; Yamaguchi, A.; Hata, K.; Ichida, F.; Meguro, H.; Aburatani, H.; Nishimura, R.; Yoneda, T. BMP2 regulates Osterix through Msx2 and Runx2 during osteoblast differentiation. *J. Biol. Chem.* **2008**, *283* (43), 29119−25.
(46) Tam, Y. Y.; Chen, S.; Cullis, P. R. Advances in Lipid Nanoparticles for siRNA Delivery. *Pharmaceutics* **2013**, *5* (3), 498−507.
(47) Wan, C.; Allen, T. M.; Cullis, P. R. Lipid nanoparticle delivery systems for siRNA-based therapeutics. *Drug Delivery Transl. Res.* **2014**, *4* (1), 74−83.

DOI: 10.1021/acsbiomaterials.5b00294
ACS Biomater. Sci. Eng. XXXX, XXX, XXX−XXX